JOURNAL OF MATERIALS SCIENCE 23 (1988) 4251–4256

Location of zinc in a conventional dental amalgam matrix

N. K. SARKAR, C. S. EYER
Department of Biomaterials, School of Dentistry, Louisiana State University, New Orleans, Louisiana 70119, USA

The location of zinc in a conventional dental amalgam matrix has been studied by electroetching, scanning electron microscopy and energy-dispersive X-ray analysis. It has been shown that zinc is randomly and non-uniformly distributed in the matrix phases. The major portion of zinc is segregated as an intergranular structure at γ_1 and γ_2 grain boundaries. A zinc-containing substructure has been observed in γ_2 but not in γ_1. A small amount of zinc may exist as solid solution in both phases.

1. Introduction

The presence of a small amount of zinc in an amalgam alloy has both beneficial and detrimental effects on the physical, mechanical and electrochemical properties of its amalgams [1]. The exact mechanism by which zinc influences these properties is not known. Since properties originate in the microstructure of a material, the information on the location of zinc in amalgam microstructure can lead to a better understanding of the structure–property relationship in this important restorative material. A number of studies on the subject have been reported previously. The location of zinc in the amalgam alloy itself is well characterized [2, 3]; however, disagreement exists as to its distribution in the matrix phases of an amalgam. According to one study [4], zinc is relatively uniformly distributed in γ_1 and γ_2. However, other studies [5–7] have indicated varying concentrations of zinc in both phases. The absence of zinc in γ_1 and γ_2 has been noted [8, 9]. The presence of zinc-containing inclusions and segregations in the matrix has also been reported [4, 8]. Considering this disagreement and the importance of zinc in amalgam properties and performance, it was felt that a re-examination of the subject would be worthwhile.

2. Materials and methods

The amalgam used in this study was made from New True Dentalloy (Batch No. 01 077 008, S. S. White Dental Manufacturing Co., Philadelphia), a commercial conventional alloy containing about 1.0 wt % Zn. Cylindrical specimens, 4 mm diameter and 6 mm long, of the amalgam were prepared using the manufacturer's recommended mercury/alloy ratio and in accordance with the American Dental Association Specification 1. The specimens were stored at 37° C for at least two weeks before surface preparation by the standard metallographic techniques. Final polishing was carried out with 0.05 μm cerium oxide.

The distribution of zinc was studied by electroetching, scanning electron microscopy and energy-dispersive X-ray analysis. Electroetching is an established metallographic technique for microstructural characterization of metals and alloys [10]. Etching of a phase or other microstructural heterogeneity such as inclusions, dislocations, grain boundaries, etc., in an alloy is accomplished by its selective dissolution in a given electrolyte at a potential where its dissolution rate is considerably greater than that of any other phase present. The choice of potentials suitable for etching zinc-containing structures in the amalgam was based on the electrochemical polarization behaviour (Fig. 1) of the amalgam in 1% NaCl solution [11]. The "break" or "re-entrant" observed in the cathodic portion of the polarization curve at around -1.3 V is associated with the oxidation of zinc. The anodic peak at around -0.95 V represents the oxidation of tin. It was rationalized that by etching of the amalgam at potentials anodic to the oxidation potential of zinc but cathodic to the oxidation potential of tin followed by microscopic examination of the surface, zinc-containing structures of the amalgam can be delineated.

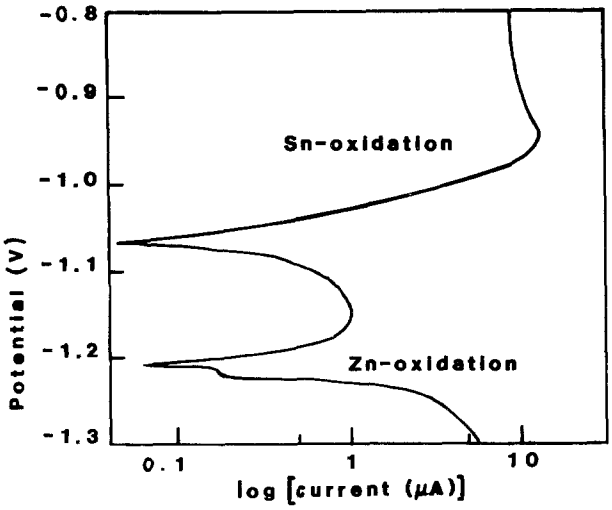

Figure 1 Potentiodynamic polarization curve of New True Dentalloy in 1% NaCl solution. Voltage measured against saturated calomel electrode.

0022–2461/88 $03.00 + .12

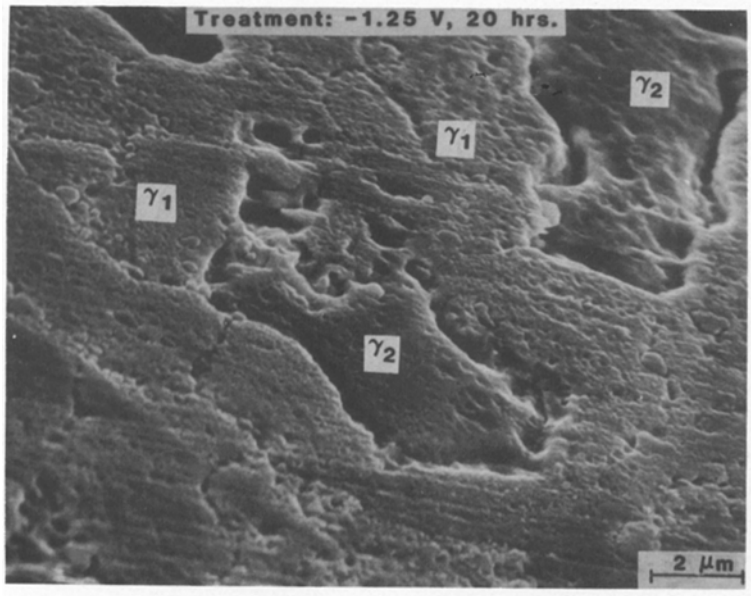

Figure 2 SEM micrograph of specimen treated at −1.25 V showing mild pitting and intergranular attack.

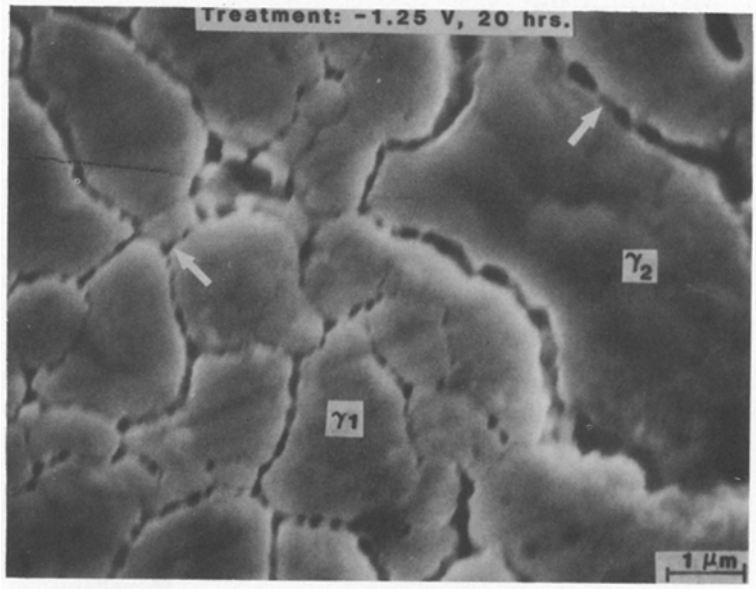

Figure 3 SEM micrograph of specimen treated at −1.25 V showing moderate intergranular attack.

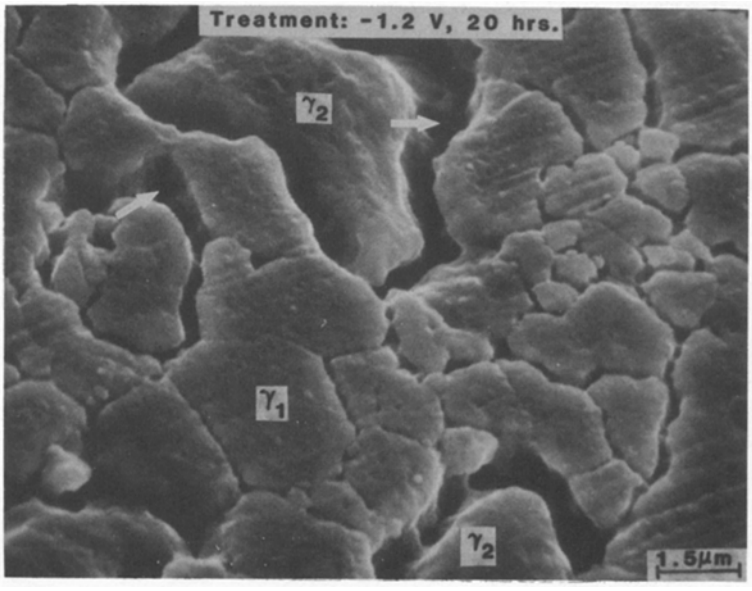

Figure 4 SEM micrograph of specimen treated at −1.2 V showing severe intergranular attack.

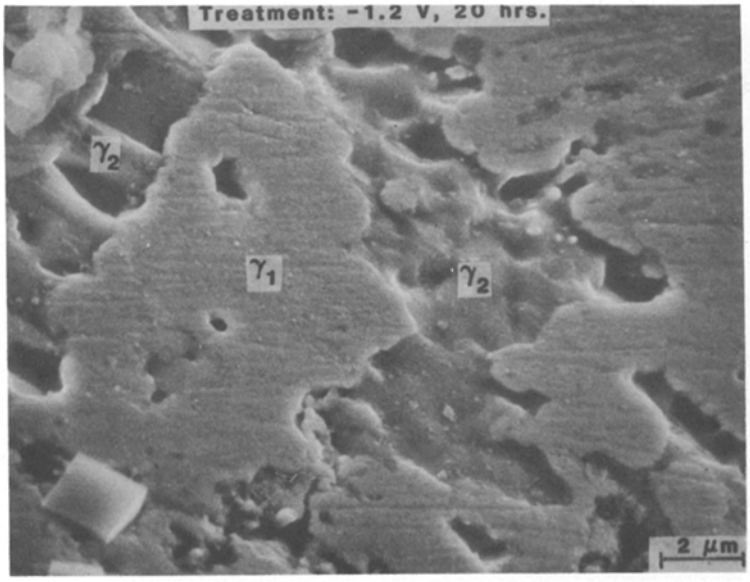

Figure 5 SEM micrograph of specimen treated at −1.2 V illustrating γ_2 intragranular attack and unattacked γ_1 and γ_2 areas.

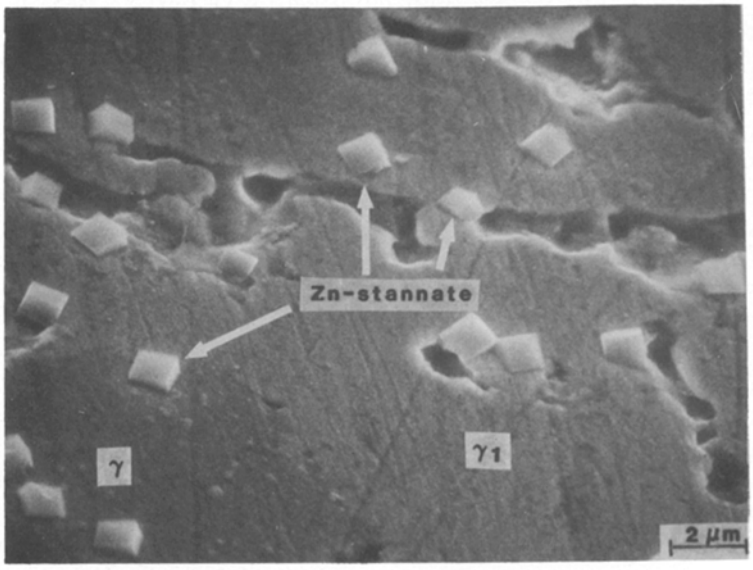

Figure 6 SEM micrograph of specimen treated at −1.2 V showing scattered zinc stannate crystals. Note also the unattacked γ_1 areas.

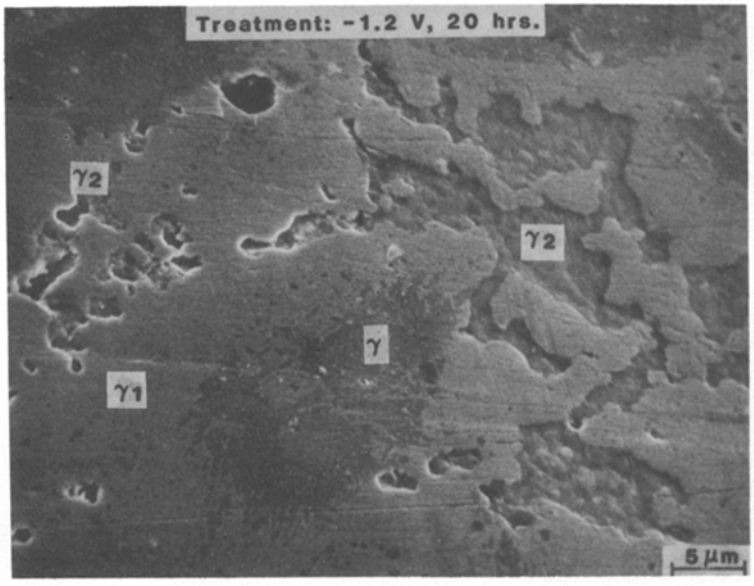

Figure 7 SEM micrograph of specimen treated at −1.2 V showing unattacked γ_1 and γ_2 and attacked γ_2 area.

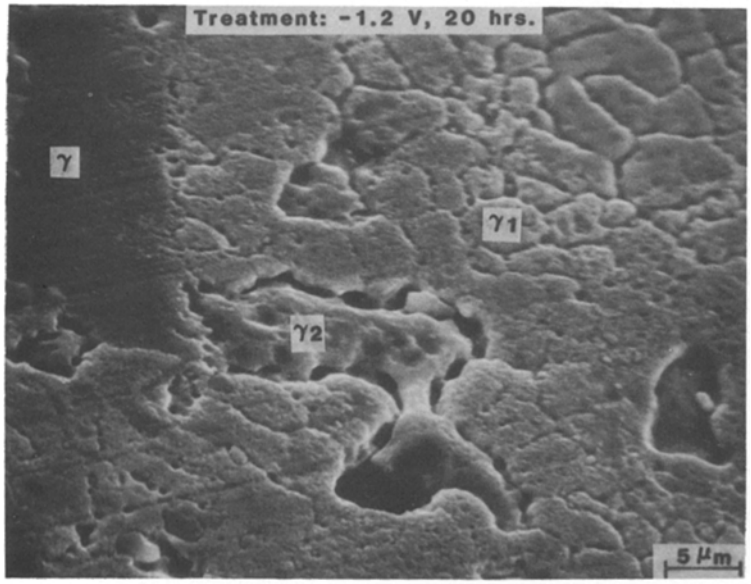

Figure 8 SEM micrograph of specimen treated at -1.2 V showing variation of the intergranular attack at different γ_1 grain boundaries.

In accordance with the above considerations, etching was carried out at -1.25 and -1.2 V for 20 h. Five specimens were treated at each potential. Following etching, the specimens were ultrasonically cleaned for 1 min in distilled water to remove any suspended oxidation products. For control, two specimens were treated at -1.3 V. Treatment at this potential leads to hydrogen evolution which cleans the surface of any oxides formed during surface preparation.

Microscopic examination of all specimens was carried out using a scanning electron microscope (SEM). Energy-dispersive X-ray analysis (EDXA) was used in conjunction with SEM to characterize the chemical nature of structures of interest.

3. Results

SEM examination of specimens etched at the two potentials showed various forms of etchant attack, namely (a) pitting, (b) intergranular corrosion and (c) intragranular attack. Typical micrographs showing these effects are presented in Figs 2 to 5. Mild pitting on the matrix and intergranular attack at or adjacent to grain boundaries of γ_1 and γ_2 were evidenced in specimens etched at -1.25 V (Figs 2 and 3). Etching at -1.2 V led to (a) severe γ_1 intergranular corrosion (Fig. 4) and (b) intragranular attack within γ_2 (Fig. 5). Crystalline deposits, identified as zinc-rich by X-ray analysis and presumably zinc-stannate, were found scattered all over the surface (Fig. 6).

It should be noted that pitting on γ_1 or its intergranular corrosion was evidenced in isolated areas but not throughout the matrix. Moreover, the severity of attack varied at different γ_1 grains and grain boundaries. The attack on γ_2, whether pitting, inter- or intra-granular, followed a similar pattern. Some γ_2 areas underwent localized or uniform attack while some others remained relatively unaffected. Additional micrographs are presented in Figs 7 and 8 to emphasize further the highly non-uniform nature of the etching effects observed in this study.

Specimens treated at -1.3 V showed no evidence of etching. The presence of a distinct grain boundary network surrounding the γ_1 grains was seen in some areas (Fig. 9). Typical X-ray analyses of the grain interior and grain boundary seen in Fig. 9 are presented in Fig. 10. While the grain interior is zinc-free (Fig. 10a), the grain boundary area (Fig. 10b) indicates the presence of significant amounts of tin and zinc in

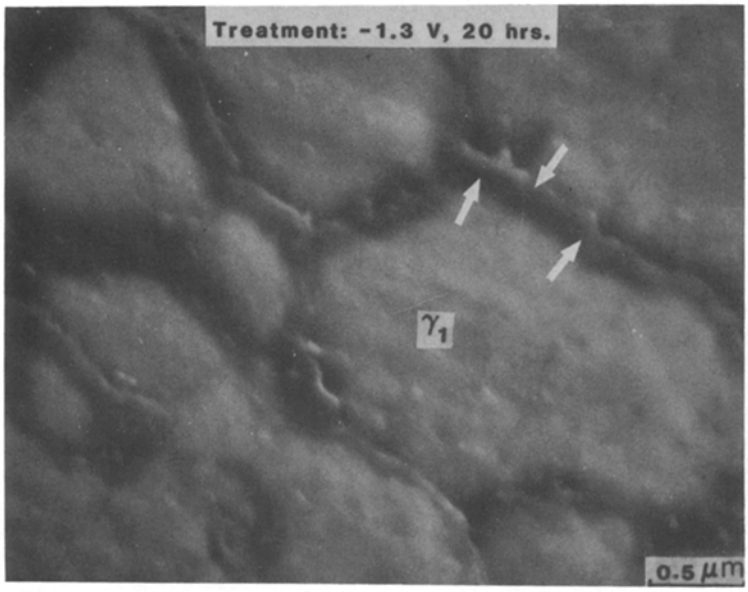

Figure 9 SEM micrograph of specimen treated at -1.25 V showing intergranular structure at γ_1 grain bondaries.

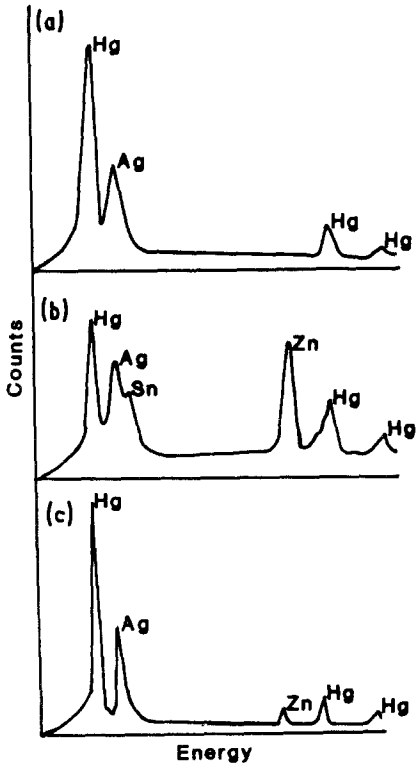

Figure 10 EDXA spectra of (a) γ_1 grain interior, (b) γ_1 grain boundary and (c) another γ_1 grain with zinc.

addition to silver and mercury which are constituents of the γ_1 phase. In some γ_1 grains, a small amount of zinc was noted (Fig. 10c).

A distinct grain boundary network (Fig. 11) was also observed in some γ_2 areas in samples treated at -1.3 V. The γ_2 area on the left-hand side of Fig. 11 is shown at a higher magnification in Fig. 12. The grain boundary was found to be zinc-rich (Fig. 13a) when compared to the interior of γ_2 (Fig. 13b). In some other areas, γ_2 was found to be associated with a sub-grain structure (Fig. 14). The X-ray analyses of some of these subgrains were found to be similar to that in Fig. 13a, suggesting that they contain zinc. The rest of the grains within the substructure of γ_2 indicated very little or no zinc and exhibited an X-ray spectrum similar to that in Fig. 13b.

It should be stressed that the intensity of the zinc line in Fig. 10b is not representative of the zinc content of all γ_1 grain boundaries. The intensity of the zinc line observed at γ_1 boundaries varied. Some grain boundaries showed a zinc concentration higher than that indicated in Fig. 10b, while zinc concentration was lower in some others. A similar variation was also noted in the zinc content of γ_2 subgrains and grain boundaries.

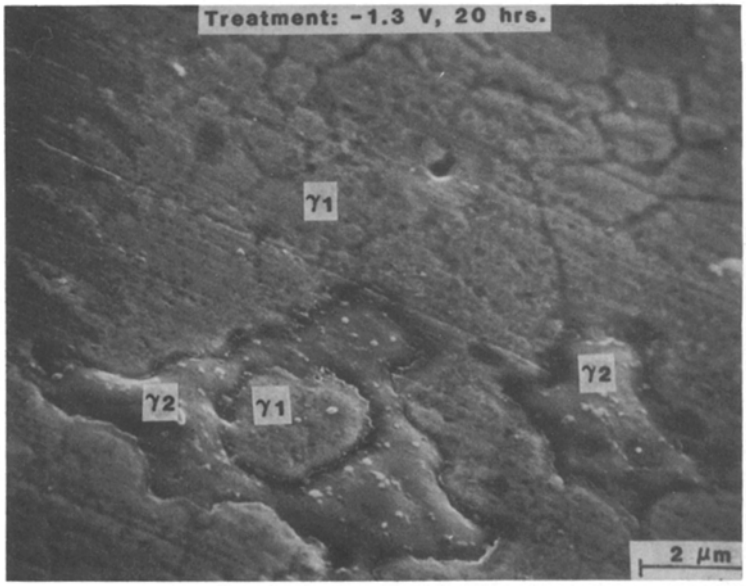

Figure 11 SEM micrograph of specimen treated at -1.3 V showing γ_2 grain boundary network. Note also the presence of a grain boundary structure surrounding some γ_1 grains.

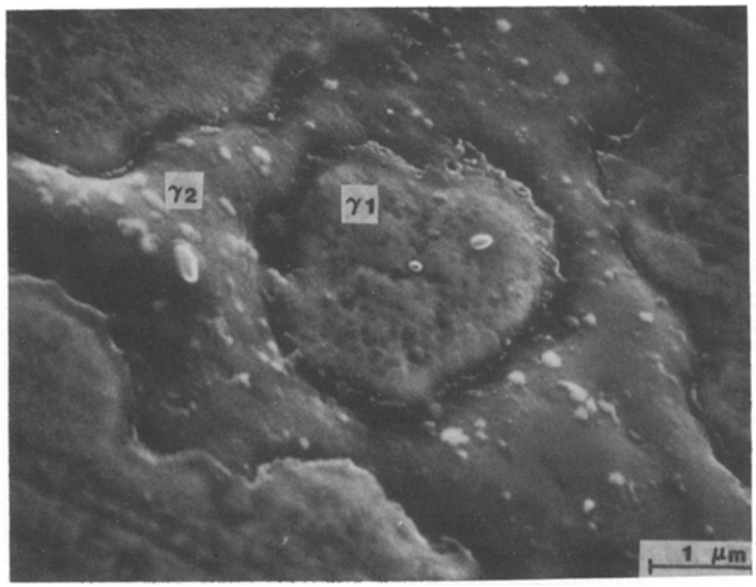

Figure 12 SEM micrograph of the γ_2 area on the left-hand side of Fig. 11.

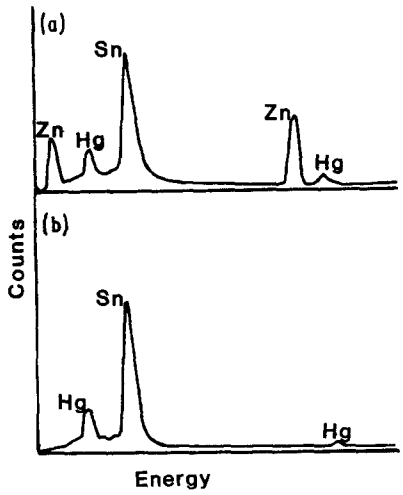

Figure 13 EDXA spectra of (a) γ_2 grain boundary and (b) γ_2 grain interior.

4. Discussion

It has been stated in the beginning that the etching potentials selected in this study are anodic to the oxidation potential of zinc but cathodic to the oxidation potential of tin. It would be reasonable to expect, then, that etching at these potentials leads to the preferential attack on those structures that contain electroactive zinc. Accordingly, areas affected by etching and showing pitting, intergranular and intergranular corrosion can be identified as structures that contained zinc.

In samples treated at -1.3 V, the presence of zinc has indeed been confirmed in those areas affected by electroetching. The intergranular attack (Figs 2 to 4) is consistent with the presence of a distinct grain boundary network (Figs 9 to 11) which is zinc-rich. The intragranular attack on γ_2 (Figs 5 to 8) can similarly be attributed to the segregation of zinc within the sub-grain structure (Fig. 14). Selective dissolution of zinc, possibly present as a solid solution in γ_1 and γ_2, appears to have contributed to pitting and consequent roughening of the matrix in selected areas.

While the preceding discussion establishes the presence of zinc in γ_1 and γ_2, the randomness with which zinc occurs in these two phases deserves further analysis. The isolated nature of the etchant attack (Figs 5 to 7) and the variation in the severity of this attack from location to location (Figs 8 and 11), as well as the variation in the intensity of the zinc X-ray line from place to place, seem to suggest that zinc is distributed in a highly haphazard and non-uniform manner in the matrix of a dental amalgam. This observation perhaps explains the disagreement that exists in the literature as to the location and distribution of zinc in amalgam matrix.

5. Conclusions

Electroetching, scanning electron microscopy and energy-dispersive X-ray analysis have shown that zinc is randomly and non-uniformly distributed in the matrix of a conventional zinc-containing dental amalgam. While a small amount of zinc may be present as a solid solution in γ_1 and γ_2, the major portion of it is segregated at γ_1 and γ_2 grain boundaries as an intergranular precipitate. A zinc-containing substructure has been observed within γ_2 but not in γ_1.

References

1. L. B. JOHNSON and G. C. PAFFENBARGER, *J. Dent. Res.* **59** (1980) 1412.
2. S. J. JENSEN, K. B. OLESEN and L. UTOFT, *Scand. J. Dent. Res.* **81** (1973) 572.
3. G. H. M. GRUBBELS, M. M. A. VRIJHOEFF and F. C. M. DRIESSENS, *J. Dent. Res.* **53** (1974) 1294.
4. L. V. SUTFIN and R. E. OGILVIE, *ibid.* **51** (1972) 1048.
5. S. J. JENSEN, P. ANDERSEN, K. B. OLESEN and L. UTOFT, *Scand. J. Dent. Res.* **83** (1975) 41.
6. D. B. MAHLER, J. D. ADEY and J. van EYSDEN, *J. Dent. Res.* **54** (1975) 218.
7. G. W. MARSHALL, S. J. MARSHALL and E. H. GREENER, *Scanning Electron Microsc.* **1** (1977) 129.
8. H. OTANI, W. A. JESSER and H. G. F. WILSDORF, *J. Biomed. Mater. Res.* **7** (1973) 523.
9. D. B. MAHLER, J. D. ADEY and J. van EYSDEN, *J. Dent. Res.* **52** (1973) 74.
10. J. A. von FRAUNHOFER and C. H. BANKS, in "Potentiostat and its Application" (Butterworths, London, 1972) p. 176.
11. N. K. SARKAR and C. EYER, *J. Dent. Res.* **61** (1982) Abstract No. 446.

Received 7 December 1987
and accepted 15 April 1988

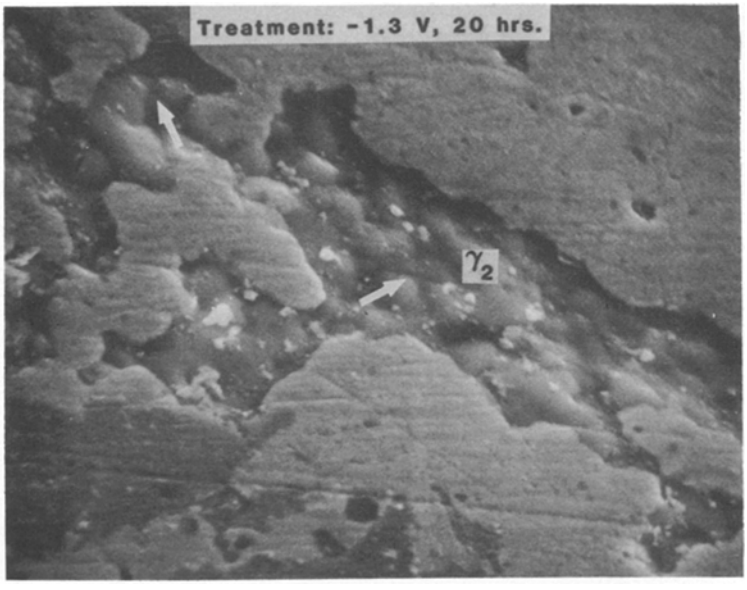

Figure 14 SEM micrograph of specimen treated at -1.3 V showing γ_2 area with sub-grain structure. Note the presence of a similar substructure of γ_2 in Fig. 7.